ISSN 1070-3632, Russian Journal of General Chemistry, 2011, Vol. 81, No. 10, pp. 2051–2061. © Pleiades Publishing, Ltd., 2011.
Original Russian Text © V.L. Stolyarova, S.I. Lopatin, O.B. Fabrichnaya, 2011, published in Zhurnal Obshchei Khimii, 2011, Vol. 81, No. 10, pp. 1597–1607.

Thermodynamic Properties of Silicate Glasses and Melts: VIII.[1] System $MgO–Al_2O_3–SiO_2$

V. L. Stolyarova[a], **S. I. Lopatin**[b], **and O. B. Fabrichnaya**[b]

[a] *St. Petersburg State University, Universitetskii pr. 26, St. Petersburg, 198504 Russia*
e-mail: stvl08@inbox.ru

[b] *Technical University of Freiberg, Institute of Sciences about Materials, Freiberg, Germany*

Received April 21, 2011

Abstract—Vaporization of the system $MgO–Al_2O_3–SiO_2$ in the temperature range 1770–1890 K was studied and activities of MgO and SiO_2 were determined. Activities of the components, isothermal sections of the phase diagram, and the position of the liquidus line in the studied system were calculated using the Gay–Kapoor–Frohberg model. The correlation of the found values of thermodynamic properties and phase equilibriua in isothermal sections of the phase diagram of the studied system was illustrated.

DOI: 10.1134/S1070363211100033

At present ceramics, refractories [2–3], glass ceramics [4], and also composite materials [5] based on the system $MgO–Al_2O_3–SiO_2$ receive increasing value among materials for new fields of engineering. Goods made from these materials possess a low and even a negative coefficient of thermal expansion [2], a high mechanical strength, and a high thermal and chemical resistance, they are good dielectrics with a wide set of properties. In the concentration range of the system $MgO–Al_2O_3–SiO_2$ compositions of the fire-proof periclase, forsterite, spinel, high-aluminous, cordierite, and mullite materials are disposed. It is necessary to note, for example, that cordierite ceramics with a low thermal expansion coefficient readily stand sharp changes in temperatures and is a rather heat-resistant material [3]. The magnesium-aluminum silicate system is a basis for glass ceramics [4], cordierite ceramics [5], metallurgical slags [7, 8], and also rocks and minerals. Since the operational use of these materials and technological processes with their participation, as a rule, proceed at high temperatures, the information on the vaporization processes, thermodynamic properties of components and phase equilibria in the system $MgO–Al_2O_3–SiO_2$ is of a significant interest.

According to the phase diagram accepted at present [9], the following crystal phases were found in the system $MgO–Al_2O_3–SiO_2$:α-$2MgO\cdot 2Al_2O_3\cdot 5SiO_2$ (cordierite), μ-$2MgO\cdot 2Al_2O_3\cdot 5SiO_2$ (crystallizes from glass below 925°C), $3MgO\ Al_2O_3\cdot 3SiO_2$ (natural pyrope), and $5MgO\cdot 6Al_2O_3\ 2SiO_2$ (natural sapphirine). Cordierite melts incongruently at 1733 K and forms a series of stable and metastable solid solutions. The compound $2MgO\cdot 2Al_2O_3\cdot 5SiO_2$ has the following polymorphic modifications: high-temperature indialite β-$2MgO\cdot 2Al_2O_3\cdot 5SiO_2$ (the synthetic species is formed above 1103 K and the natural, in a lava), low-temperature indialite β-$2MgO\cdot 2Al_2O_3\cdot 5SiO_2$ (the synthetic species is formed below 1103 K), high-temperature cordierite (in vulcanics), low-temperature cordierite (in igneous rock), μ-$Mg_2Al_4Si_5O_{18}$ (formed by a synthesis in the temperature range 1123-1173 K), and osumilite (in vulcanics). Phase equallibria in various sections of the system under study were studied in the works [10, 11]. At 1873 K in the system $MgO–Al_2O_3–SiO_2$ the presence of an immiscibility area was found [12]. Glass-formation processes and corresponding concentration ranges in the magnesium-aluminum silicate system were studied in detail in the works [13, 14].

Available experimental data on the thermodynamic properties of the system $MgO–Al_2O_3–SiO_2$ at high temperatures are not numerous. They are mainly limited to the results of studying the system under consideration by the methods of exchange equilibria [15, 16], high-temperature calorimetry of dissolution

---

[1] For communication VII, see [1].

[17, 18], differential scanning calorimetry [19, 20], and high-temperature mass spectrometry [21, 22].

Activity of silicon dioxide in the system MgO–Al_2O_3–SiO_2 was determined at 1873 K in [15] from the silicon distribution between slags of the system under study and Fe–Si–C alloys saturated with graphite or silicon carbide. The activity of silicon dioxide in MgO–Al_2O_3–SiO_2 melts at 1723 and 1773 K was found by measuring the equilibrium pressure of CO in reaction (1) [16].

$$SiO_2(\text{cr.}) + 3C(\text{cr.}) = SiC(\text{cr.}) + 2CO(\text{gas}). \quad (1)$$

Enthalpies of sapphirine and $(MgSiO_3)_{0.9}(Al_2O_3)_{0.1}$ formation from oxides were determined at 970 K by high-temperature calorimetry of dissolution using a $2PbO{\cdot}SiO_2$ melt as a solvent [17]. The same method was applied to obtain enthalpies of formation of glasses in the system MgO–Al_2O_3–SiO_2 [18]. The temperature dependences of heat capacity, and also values of the enthalpy of formation and entropy of sapphirine at standard conditions were obtained by the calorimetry method [19]. Values of cordierite heat capacity in the temperature range 330–950 K were determined in [20].

Results of studying vaporization processes and thermodynamic properties of MgO–Al_2O_3, Al_2O_3–SiO_2, and MgO–SiO_2 binary mixtures as constituents of the triple system under study were summarized in the monograph [23]. The thermodynamic data found in the recent works by studying the systems Al_2O_3–SiO_2 [24–29] and MgO–SiO_2 [30–33] by high-temperature mass-spectrometry are compatible and correlate with the information on phase equilibria in the specified systems.

The composition of vapor in the system $MgAl_2O_4$–SiO_2 was studied in [21], and activities of the components were determined in the temperature range 1623–2523 K by the Belton–Fruechan method [34]. As the values of intensities of SiO^+, Mg^+, and Al^+ ionic currents entering into the equations for calculation of the activities differed by more than two orders, the obtained data cannot be treated as reliable. In [22] the composition of vapor above the system MgO–Al_2O_3–SiO_2 was studied, and Gibbs energies of formation in melts of this system at 1890 K were determined, and also thermodynamic properties were simulated on the basis of the generalized lattice theory of associated solutions. Thermodynamic properties of glass-forming melts of the system MgO–Al_2O_3–SiO_2 can be described within the limits of this approach.

Activities of components of slags of the system MgO–Al_2O_3–SiO_2 at 1873 K in the area of compositions typical for the production of single-stage ferrosilicochromium were calculated by the methods of Fllod-Johnston, Kozhurov, and Ponomarenko [35]. It was found that the activity of silicon oxide decreases as the ratio of concentrations [MgO]:[Al_2O_3] varies from 1:1 up to 25:1, and also as temperature increases.

Thermodynamic properties of solid solutions in the system $Mg_3Al_2Si_3O_{12}$–$Mg_4Si_4O_{12}$ in the temperature range 1073–3673 K and pressure range 0–20 hPa were recently calculated with the use of a spatially-cluster model by the Monte-Carlo method [36].

Careful and detailed optimization of parameters on the basis of available experimental data on the phase equilibria and thermodynamic functions in the system MgO–Al_2O_3–SiO_2 was fulfilled in the works [37–39]. Solid solutions in the system under study were described within the limits of the sublattice model [40]. The physicochemical description of melts of the system MgO–Al_2O_3–SiO_2 was fulfilled within the limits of the modified quasichemical model [37], the sublattice model of ionic liquid [38], and the Gay–Kapoor–Frohberg model (a variety of the quasichemical model) [39]. It is necessary to emphasize that phase equilibria in the system MgO–Al_2O_3–SiO_2 calculated in the works [37–39] for a wide temperature interval satisfactorily agree with the experimental data accepted at present [16]. It was found that the SiO_2 activities in melts of the system MgO–Al_2O_3–SiO_2 calculated with the use of all above-mentioned models agree acceptably with the experimental data [16] for the temperatures 1773 and 1823 K. At the same time the results of experimental determination of the silicon dioxide activity in melts of the system under consideration at 1873 K obtained in [15] were reproduced in the calculations [37–39] insufficiently. Therefore necessity of the further experimental research for the determination of activities of components in melts of the system MgO–Al_2O_3–SiO_2 was emphasized [38].

Vaporization processes in the system MgO–Al_2O_3–SiO_2 were studied by high-temperature mass-spectrometry and activities of the components were determined for the temperature range of 1770–1890 K, the range of compositions from 10 up to 90 mol % of SiO_2, and the ratios of molar concentrations [MgO]:[Al_2O_3] of 2.33, 1.00, 0.43, and 0.18.

The X-ray analysis has shown that the contents of the main components in samples of the system MgO–

Table 1. Values of ionic current intensities (I_i^+, relative units) measured in mass spectra of vapor above the system MgO–Al_2O_3–SiO_2 at the ratio of MgO and Al_2O_3 mole fractions 2.33 and above the standard, and also values of MgO and SiO_2 activities (a_i) at 1770, 1820, and 1890 K

Sample composition, [MgO]:[Al_2O_3]:[SiO_2], mol %	T, K	Sample				Standard				Activity, a_i	
		SiO^+	Mg^+	MoO_3^+	MoO_2^+	SiO^+	Mg^+	MoO_3^+	MoO_2^+	MgO	SiO_2
7:3:90	1770	19.0	0.7	0.9	0.5	18.0	1.4	1.4	0.7	5.6×10^{-2}	0.95
	1820	174.0	1.4	10.5	5.1	205.0	2.8	11.7	6.3	5.4×10^{-2}	0.94
	1890	350.0	2.2	22.0	14.0	366.0	3.6	31.0	19.0	4.8×10^{-2}	0.92
14:6:80	1770	20.0	0.3	1.2	0.7	17.2	0.6	1.9	0.9	5.4×10^{-2}	0.94
	1820	65.0	0.4	5.4	2.7	79.0	1.2	12.0	6.9	5.2×10^{-2}	0.95
	1890	150.0	0.8	14.1	8.4	176.0	1.6	35.0	22.0	5.4×10^{-2}	0.90
21:9:70	1770	20.0	0.5	1.2	0.6	23.0	1.0	1.9	1.0	6.1×10^{-2}	0.92
	1820	72.0	0.8	5.0	2.1	100.0	2.5	11.4	6.0	5.3×10^{-2}	0.90
	1890	280.0	2.4	16.2	9.0	360.0	4.9	35.0	22.0	5.6×10^{-2}	0.88
35:15:50	1770	29.0	0.7	0.9	0.7	52.0	0.7	1.8	1.2	0.13	0.48
	1820	90.0	2.3	3.9	2.1	133.0	3.7	8.1	5.7	0.13	0.47
	1890	190.0	6.6	12.6	9.6	405.0	9.2	22.5	17.1	0.15	0.47
42:18:40	1770	30.0	2.4	0.87	0.4	70.0	1.3	3.0	1.6	0.30	0.44
	1820	53.0	5.2	3.1	2.0	116.0	3.8	6.6	4.2	0.33	0.45
	1890	228.0	17.3	14.4	11.4	486.0	8.4	22.0	16.0	0.34	0.43
49:21:30	1770	12.3	2.3	0.6	0.4	21.0	2.4	4.9	1.0	0.40	0.46
	1820	48.0	7.8	4.5	2.9	107.0	12.8	5.1	3.3	0.39	0.45
	1890	123.0	24.0	12.3	9.3	296.0	36.9	15.3	11.7	0.42	0.42
63:27:10	1770	13.0	1.7	0.7	0.3	48.0	4.0	2.0	1.2	0.45	0.38
	1820	89.0	6.0	4.2	2.4	288.0	14.3	13.5	8.1	0.44	0.37
	1890	340.0	25.0	11.7	8.1	976.0	58.2	43.0	30.0	0.42	0.35

Al_2O_3–SiO_2 correspond to the charge composition with an accuracy of no less than 0.5 mol %.

The ions SiO^+, Mg^+, MgO^+, MoO_3^+, and Mo_2^+ were identified in the mass spectra of vapor above samples of the system MgO–Al_2O_3–SiO_2 in the temperature range 1770–1940 K in proportions depending on the composition of a condensed phase and temperature. To determine the nature of ions in the vapor above the system under study, we have measured appearance energies of ions by the method of disappearing ionic current (standard - gold with the ionization energy of 9.22 eV [41]), which appeared to be (±0.3 eV): Mg^+ 7.6, SiO^+ 10.6, MoO_2^+ 9.5, and MoO_3^+ 12.1 eV. We did not measure the appearance energy of the MgO^+ ion because of a low intensity of the ionic current. All ions detected in the mass spectrum of vapor above the system MgO–Al_2O_3–SiO_2 are molecular, as the effecttiveness curves of ionization contain no inflections, and their appearance energies coincide within the limits of measuring errors with the ionization energies of the corresponding molecules [41]. At a stepwise increase in temperature and the subsequent isothermal holding ionic currents of SiO^+ and Mg^+ gradually decreased. After complete removal of SiO_2 from the samples and temperature rise up to 2100 K the ions Al^+, AlO^+, and Al_2O^+ with appearance energies corresponding to the ionization energies of the corresponding molecules started to be fixed in the vapor [41].

The dependence of the vapor mass spectra on temperature, composition of a condensed phase, and vaporization time and also the values of appearance energies of the ions testify that SiO^+, atomic magnesium, oxygen, and products of reaction of samples with a cell material, MoO_3 and MoO_2 oxides, are present in vapor above the studied ternary system in the temperature range 1770–1940 K. At isothermal vaporization the condensed phase is gradually depleted of the most volatile component, silicon dioxide, and is enriched in magnesium and aluminum oxides. Later on, after complete removal of silicon dioxide and temperature rise up to 2100–2200 K atomic aluminum

Table 2. Values of ionic current intensities (I_i^+, relative units) measured in mass spectra of vapor above the system MgO–Al_2O_3–SiO_2 at the ratio of MgO and Al_2O_3 mole fractions 1.00 and above the standard, and also values of MgO and SiO_2 activities (a_i) at 1770, 1820, and 1890 K

Sample composition, [MgO]:[Al_2O_3]:[SiO_2], mol %	T, K	Sample				Standard				Activity, a_i	
		SiO^+	Mg^+	MoO_3^+	MoO_2^+	SiO^+	Mg^+	MoO_3^+	MoO_2^+	MgO	SiO_2
5:5:90	1770	44.0	0.3	1.9	0.9	50.0	0.8	2.9	1.5	3.4×10^{-2}	0.95
	1820	174.0	0.9	11.4	6.6	182.0	2.0	13.2	7.5	3.4×10^{-2}	0.94
	1890	270.0	0.8	25.0	13.0	296.0	1.6	28.4	14.9	3.3×10^{-2}	0.92
10:10:80	1770	24.6	0.2	2.0	1.0	27.3	0.6	2.7	1.4	2.7×10^{-2}	0.94
	1820	96.0	0.3	3.4	1.8	105.0	0.8	4.5	2.4	2.8×10^{-2}	0.92
	1890	240.0	2.1	10.2	5.4	260.0	4.2	11.7	6.0	3.0×10^{-2}	0.89
15:15:70	1770	26.0	0.3	2.6	1.3	32.0	0.8	2.3	1.3	4.0×10^{-2}	0.92
	1820	123.0	0.7	4.5	2.2	155.0	1.5	5.4	3.0	4.0×10^{-2}	0.90
	1890	270.0	2.3	9.0	4.8	307.0	3.3	15.0	8.1	4.3×10^{-2}	0.89
25:25:50	1770	17.5	0.5	2.0	0.8	35.0	0.9	2.3	1.0	6.8×10^{-2}	0.54
	1820	40.0	0.9	4.2	2.1	82.0	1.6	5.4	3.0	5.9×10^{-2}	0.54
	1890	260.0	3.3	17.1	8.7	478.0	3.4	37.0	18.0	6.7×10^{-2}	0.52
30:30:40	1770	12.5	0.4	1.4	0.7	21.0	1.2	2.6	1.2	3.2×10^{-2}	0.55
	1820	39.0	0.7	2.8	1.5	86.0	2.1	9.6	6.0	3.5×10^{-2}	0.53
	1890	140.0	2.3	5.7	3.6	265.0	4.5	23.0	14.0	3.6×10^{-2}	0.51
35:35:30	1770	13.0	0.5	0.4	0.2	28.0	0.7	0.4	0.2	9.0×10^{-2}	0.50
	1820	42.0	1.7	3.0	1.6	100.0	2.1	10.2	6.3	9.0×10^{-2}	0.48
	1890	138.0	2.8	7.2	4.2	302.0	2.3	24.0	15.0	0.10	0.49
45:45:10	1770	6.8	3.6	0.4	0.2	24.3	3.0	1.3	0.7	0.16	0.33
	1820	33.0	7.5	3.9	2.4	99.0	4.2	10.8	6.6	0.17	0.33
	1890	90.0	9.3	7.5	4.5	286.0	4.3	25.1	15.3	0.17	0.32

Table 3. Values of ionic current intensities (I_i^+, relative units) measured in mass spectra of vapor above the system MgO–Al_2O_3–SiO_2 at the ratio of MgO and Al_2O_3 mole fractions 0.43 and above the standard, and also values of MgO and SiO_2 activities (a_i) at 1770, 1820, and 1890 K

Sample composition, [MgO]:[Al_2O_3]:[SiO_2], mol %	T, K	Sample				Standard				Activity, a_i	
		SiO^+	Mg^+	MoO_3^+	MoO_2^+	SiO^+	Mg^+	MoO_3^+	MoO_2^+	SiO^+	Mg^+
3:7:90	1770	271.0	0.3	6.9	3.6	246.0	3.0	13.5	6.3	1.1×10^{-2}	0.99
	1820	390.0	0.6	31.2	17.5	314.0	4.2	50.3	22.4	1.1×10^{-2}	0.99
	1890	428.0	0.8	78.0	27.9	553.0	5.8	79.1	35.0	1.3×10^{-2}	0.96
6:14:80	1770	207.0	0.3	16.0	8.7	210.0	2.7	18.0	9.6	1.2×10^{-2}	0.97
	1820	416.0	0.5	33.0	17.4	390.0	4.0	42.0	20.0	1.2×10^{-2}	0.96
	1890	510.0	1.0	69.0	38.0	510.0	5.4	87.0	45.0	1.4×10^{-2}	0.94
9:21:70	1770	210.0	0.5	18.9	9.6	213.0	3.1	15.0	7.2	1.8×10^{-2}	0.94
	1820	342.0	0.9	39.0	20.1	354.0	4.7	42.6	21.0	1.9×10^{-2}	0.93
	1890	547.0	1.6	75.3	40.0	526.0	5.9	71.5	34.2	2.0×10^{-2}	0.90
15:35:50	1770	66.0	0.2	9.0	4.5	100.0	0.8	20.0	9.2	2.5×10^{-2}	0.61
	1820	120.0	0.3	22.0	10.0	193.0	1.1	37.9	16.4	2.7×10^{-2}	0.59
	1890	200.0	0.7	42.0	18.8	387.0	1.9	69.5	32.0	3.0×10^{-2}	0.58
18:42:40	1770	37.3	0.1	4.8	2.4	67.7	1.4	10.4	5.1	3.1×10^{-2}	0.54
	1820	205.0	0.4	13.8	7.2	203.0	4.1	38.5	20.0	2.8×10^{-2}	0.52
	1890	384.0	1.9	25.4	15.0	580.0	0.5	120.0	57.0	3.0×10^{-2}	0.53

Table 3. (Contd.)

Sample composition, $[MgO]:[Al_2O_3]:[SiO_2]$, mol %	T, K	Sample				Standard				Activity, a_i	
		SiO^+	Mg^+	MoO_3^+	MoO_2^+	SiO^+	Mg^+	MoO_3^+	MoO_2^+	SiO^+	Mg^+
21:49:30	1770	72.0	0.3	7.2	4.2	122.3	0.8	18.4	10.0	3.9×10^{-2}	0.55
	1820	258.0	1.3	27.0	17.0	392.0	2.3	76.1	39.2	4.5×10^{-2}	0.54
	1890	439.0	4.9	68.0	40.0	598.0	5.7	182.0	75.8	4.9×10^{-2}	0.52
27:63:10	1770	52.0	0.6	2.5	1.7	140.8	1.0	16.9	8.5	5.2×10^{-2}	0.27
	1820	138.0	1.3	11.1	7.8	377.0	1.9	52.3	24.6	4.6×10^{-2}	0.25
	1890	380.0	3.6	31.2	29.5	992.0	4.8	113.0	66.9	4.0×10^{-2}	0.24

Table 4. Values of ionic current intensities (I_i^+, relative units) measured in mass spectra of vapor above the system MgO–Al_2O_3–SiO_2 at the ratio of MgO and Al_2O_3 mole fractions 0.18 and above the standard, and also values of MgO and SiO_2 activities (a_i) at 1770, 1820, and 1890 K

Sample composition, $[MgO]:[Al_2O_3]:[SiO_2]$, mol %	T, K	Sample				Standard				Activity, a_i	
		SiO^+	Mg^+	MoO_3^+	MoO_2^+	SiO^+	Mg^+	MoO_3^+	MoO_2^+	MgO	SiO_2
1.5:8.5:90	1770	44.0	0.1	0.6	0.3	21.0	2.4	0.7	0.4	7.0×10^{-3}	0.98
	1820	174.0	0.2	3.2	2.4	58.0	2.2	4.5	3.9	8.0×10^{-3}	0.96
	1890	270.0	0.1	7.8	6.0	195.0	0.8	20.4	14.4	8.0×10^{-3}	0.97
3:17:80	1770	24.6	0.2	0.5	0.2	19.0	2.6	0.39	0.2	9.0×10^{-3}	0.94
	1820	96.0	0.1	8.1	4.2	150.0	1.2	21.0	11.4	8.0×10^{-3}	0.95
	1890	240.0	0.1	17.0	11.0	273.0	0.7	52.0	29.1	9.0×10^{-3}	0.92
4.5:25.5:70	1770	26.0	0.1	0.5	0.3	20.0	1.0	0.6	0.3	1.1×10^{-2}	0.94
	1820	123.0	0.1	4.9	3.1	89.0	0.6	5.1	2.7	9.0×10^{-3}	0.92
	1890	270.0	0.1	9.0	6.0	154.0	0.8	12.1	7.0	1.1×10^{-2}	0.90
7.5:42.5:50	1770	17.5	0.2	0.7	0.4	37.0	1.3	0.8	0.4	1.9×10^{-2}	0.48
	1820	40.0	0.4	7.2	4.5	370.0	1.9	24.0	12.6	2.0×10^{-2}	0.47
	1890	260.0	1.2	32.0	25.0	1040.0	3.9	80.0	48.0	1.9×10^{-2}	0.45
9:51:40	1770	12.5	0.1	0.5	0.2	62.0	0.5	1.6	0.7	2.9×10^{-2}	0.46
	1820	39.0	0.2	2.2	1.1	270.0	1.0	13.9	6.9	2.7×10^{-2}	0.46
	1890	140.0	1.0	15.0	9.9	686.0	3.2	53.0	33.0	3.0×10^{-2}	0.44
10.5:59.5:30	1770	13.0	0.1	0.5	0.2	83.0	0.3	1.6	0.8	4.6×10^{-2}	0.45
	1820	42.0	0.4	3.5	2.6	286.0	0.9	17.7	10.2	4.5×10^{-2}	0.44
	1890	138.0	0.9	14.7	10.2	487.0	1.5	44.0	24.0	4.7×10^{-2}	0.42
13.5:76.5:10	1770	6.8	0.2	0.5	0.5	60.0	0.4	1.6	0.9	4.5×10^{-2}	0.28
	1820	33.0	1.0	2.7	1.9	496.0	5.8	9.0	6.9	4.5×10^{-2}	0.28
	1890	90.0	3.0	13.2	9.9	1162.0	10.8	26.0	18.0	4.6×10^{-2}	0.27

and AlO and Al_2O oxides appear in the vapor. Owing to differences in volatilities of magnesium and aluminum oxides the system is depleted of magnesium oxide and enriched in aluminum oxide at isothermal holding.

Activities of MgO and SiO_2 were determined using Eqs. (2) and (3), respectively.

$$a(MgO) = p(MgO)/p^0(MgO), \quad (2)$$

$$a(SiO_2) = p(SiO_2)/p^0(SiO_2). \quad (3)$$

Reactions of silicon dioxide and magnesium oxide dissociation and also reactions of oxygen with a cell material can we written as Eqs. (4)–(7).

$$SiO_2(\text{cr., l.}) = SiO(\text{gas}) + 0.5O_2(\text{gas}), \quad (4)$$

$$MgO(\text{cr.}) = Mg(\text{gas}) + 0.5O_2(\text{gas}), \quad (5)$$

$$Mo(\text{cr.}) + O_2(\text{gas}) = MoO_2(\text{gas}), \quad (6)$$

$$Mo(\text{cr.}) + 1.5O_2(\text{gas}) = MoO_3(\text{gas}). \quad (7)$$

Partial pressures of molybdenum oxides and atomic and molecular oxygen are related to each other by Eqs. (8) and (9).

$$MoO_3(gas) = MoO_2(gas) + O(gas), \qquad (8)$$

$$O_2(gas) = 2O(gas). \qquad (9)$$

It allows us to replace partial pressures of the vapor molecular species by intensities of ionic currents, which are proportional to them, and thus to obtain Eqs. (10) and (11).

$$a(SiO_2) = p(SiO)p(O)/p^0(SiO)p^0(O) = I(SiO)I(O)/I^0(SiO)I^0(O), \qquad (10)$$

$$a(MgO) = p(Mg)p(O)/p^0(Mg)p^0(O). \qquad (11)$$

Here p and I, p^0 and I^0 are related, respectively, to partial pressures and intensities of ionic currents in vapor and in a mass spectrum of vapor above the studied sample and individual oxide. It is practically impossible to measure intensities of ionic currents of O^+ or O_2^+, which are proportional to partial pressures of atomic and molecular oxygen in vapor above the studied samples and the standard, because of the presence of a high hum noise at m/z 16 and 32. Therefore we have replaced the partial pressure of elemental oxygen in Eqs. (10) and (11) by the ratio of partial pressures of molybdenum oxides according to Eq. (12), where $p(O)$ is expressed in terms of equilibrium constant of gas-phase reaction (8).

$$p(O) = K_{eq}p(MoO_3)/p(MoO_2). \qquad (12)$$

The presence of the ions SiO^+, Mg^+, MoO_3^+, and MoO_2^+ in the mass spectra of vapor above the studied samples of the system $MgO–Al_2O_3–SiO_2$ at 1770–1890 K allowed us to determine simultaneously activities of magnesium oxide and silicon dioxide. We used the system of 10 mol % MgO, 90 mol % SiO_2 as the standard of activities of the components, for which activities of magnesium and silicon oxides have been measured earlier [30, 31] with a high reliability.

As a result activities of MgO and SiO_2 were determined according to Eqs. (13) and (14).

$$a(MgO) = \{a^*(MgO)[I(Mg)^+/I^*(Mg)^+]\} \times \{[I(MoO_3)^+/I(MoO_2)^+]\,[I^*(MoO_2)^+/I^*(MoO_3)^+]\}, \qquad (13)$$

$$a(SiO_2) = \{a^*(SiO_2)[I(SiO)^+/I^*(SiO)^+]\} \times \{[I(MoO_3)^+/I(MoO_2)^+]\,[I^*(MoO_2)^+/I^*(MoO_3)^+]\}. \qquad (14)$$

Here a_i, a_i^*, I_i, and I_i^* are activities of the ith component and intensities of ionic currents in the mass spectra of vapor above the systems $MgO–Al_2O_3–SiO_2$ and 10 mol % MgO, 90 mol % SiO_2, respectively. The results of the determination of activities of magnesium and silicon oxides at 1770, 1820, and 1890 K are given in Tables 1–4.

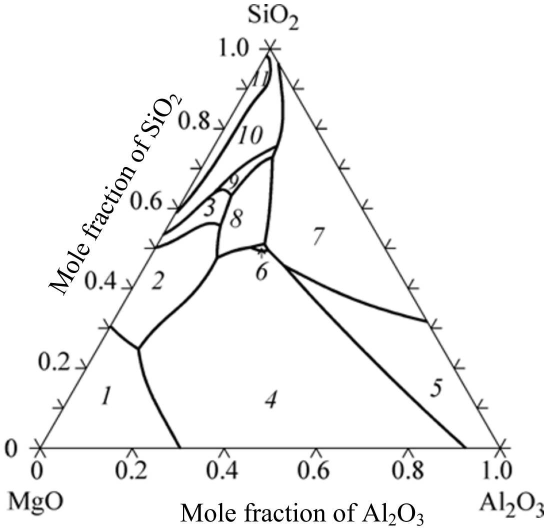

Fig. 1. Liquidus surface of the system $MgO–Al_2O_3–SiO_2$ calculated in the present work. (*1*) MgO, (*2*) olivine, (*3*) protoenstatite, (*4*) spinel, (*5*) Al_2O_3, (*6*) sapphirine, (*7*) mullite, (*8*) cordierite, (*9*) tridymite, and (*10*) cristobalite.

The error in the determination of SiO_2 and MgO activities in the system $MgO–Al_2O_3–SiO_2$ is the sum of the errors of measuring intensities of SiO^+, Mg^+, MoO_2^+, and MoO_3^+ ionic currents. As the intensities of SiO^+, MoO_2^+, and MoO_3^+ ionic currents in the mass spectra of vapor above the system under study were rather high, the error of measuring SiO_2 activity did not exceed 10%. The values of MgO activity in the system $MgO–Al_2O_3–SiO_2$ were determined with an essentially greater error exceeding 100% in separate measurings, which is connected with low values of the intensities of Mg^+ ionic current in the mass spectra of vapor above the system under study.

To consider mutual agreement of the values of MgO and SiO_2 activities in the system $MgO–Al_2O_3–SiO_2$ found in this work with the phase equilibria in this system, we have calculated a liquidus surface and isothermal sections of the phase diagram of this system using the thermodynamic database [39].

As earlier, we described solid solutions of the system under study by the sublattice model [40]. Analytical dependences of the Gibbs energy for solid phases in the three-component system under consideration were taken from the descriptions of the binary systems $MgO–SiO_2$ [42], $Al_2O_3–SiO_2$ [43], and

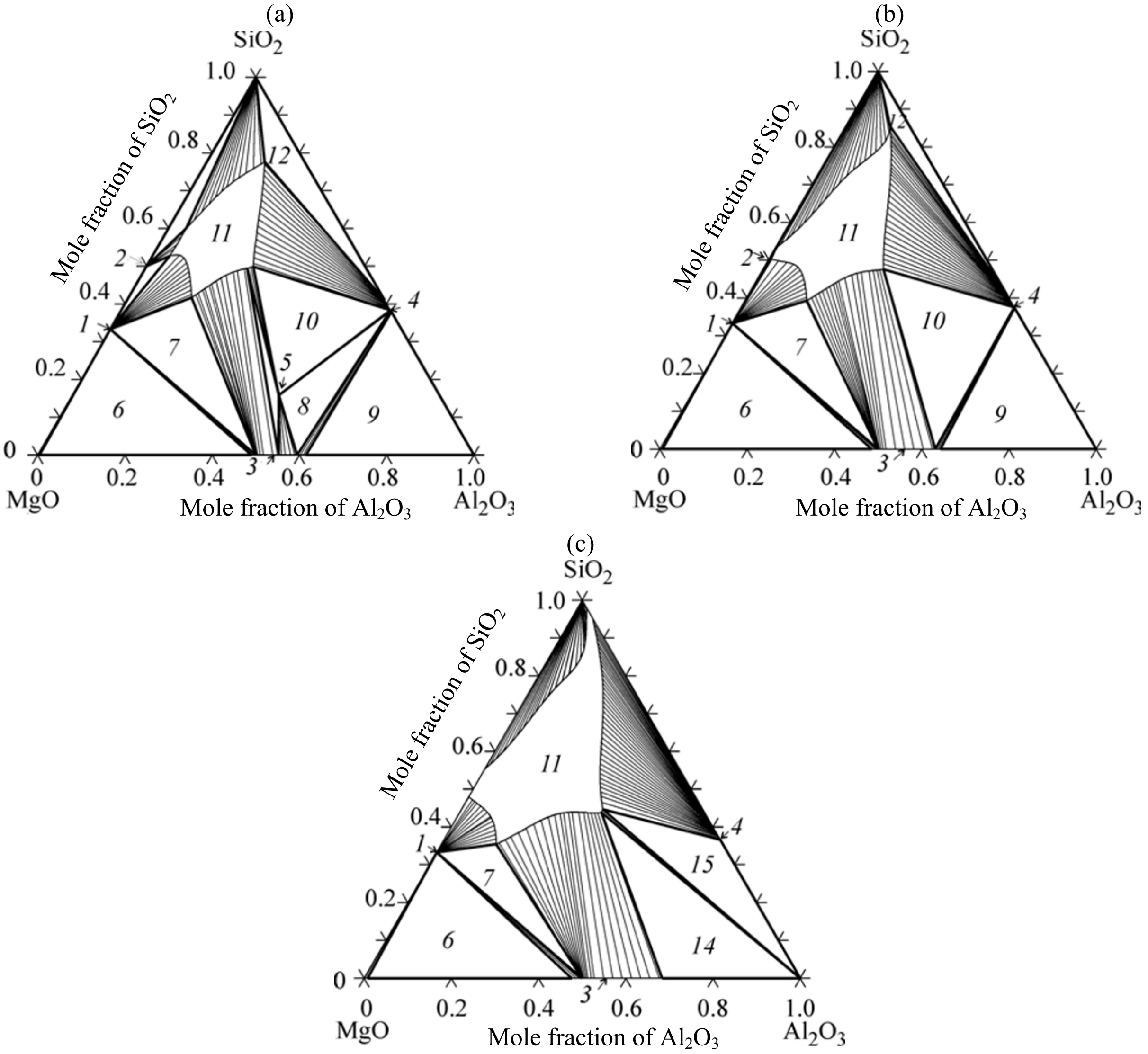

Fig. 2. Isothermal sections of the phase diagram of the system $MgO–Al_2O_3–SiO_2$ at (a) 1770, (b) 1820, and (c) 1890 K calculated in the present work. (*1*) Olivine, (*2*) protoenstatite, (*3*) spinel, (*4*) mullite, (*5*) sapphirine, (*6*) MgO–spinel–olivine, (*7*) olivine–spinel–mullite, (*8*) sapphirine–spinel–mullite, (*9*) mullite–Al_2O_3–spinel, (*10*) melt–sapphirine–mullite, (*11*) melt, (*12*) cristobalite–mullite–melt, (*13*) spinel–mullite–melt, (*14*) spinel–Al_2O_3–melt, and (*15*) mullite–Al_2O_3–melt.

$MgO–Al_2O_3$ [44]. The ternary compounds sapphirine and cordierite were considered as stoichiometric. Behavior of melts of the system $MgO–Al_2O_3–SiO_2$ was described by the Gay–Kapoor–Frohberg model [45, 46]. It is necessary to note that we used experimental data on the position of a liquidus line summarized in [9] to optimize parameters of the interaction between particles of the system $MgO–Al_2O_3–SiO_2$ melts, whereas the results of the experimental determination of activities of the components obtained both in [15, 16] and in the present work were not taken into consideration. Therefore, the comparison of the experimental values of MgO and SiO_2 activities in the system $MgO–Al_2O_3–SiO_2$ obtained in the present work is the important check of the consistency of a thermodynamic database [39] with the experiment.

The liquidus surface of the system $MgO–Al_2O_3–SiO_2$ calculated in the present work is shown in Fig. 1.

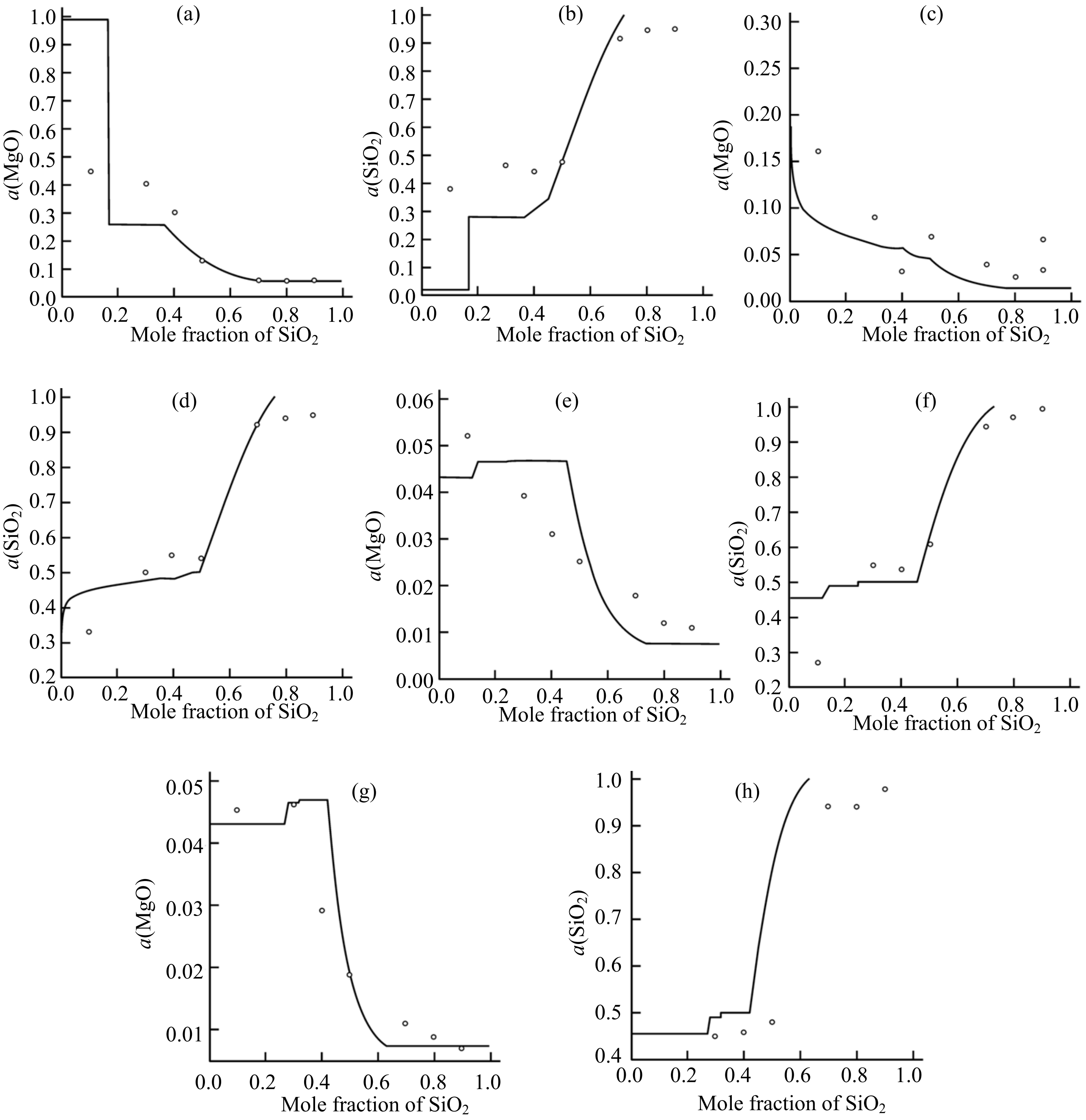

Fig. 3. Values of activities of (a, c, e, g) MgO and (b, d, f, h) SiO_2 in the system $MgO–Al_2O_3–SiO_2$ at ratios of MgO and Al_2O_3 mole fractions (a, b) 2.33, (c, d) 1.00, 0.43, 0.18 (1770 K) found in the present work. (Circles) experimental values, (lines) results of calculation within the limits of the Gay–Kapoor–Frohberg model.

The isothermal sections of the phase diagram under study calculated at temperatures 1770, 1820, and 1890 K are presented in Figs. 2a–2c.

Concentration dependences of MgO and SiO_2 activities in the system $MgO–Al_2O_3–SiO_2$ at fixed $MgO–Al_2O_3$ molar ratios at 1770 and 1890 K, respectively, were obtained experimentally in the present work and calculated within the limits of the approach described above for the first time. They are compared in Figs. 3a–3h and Figs. 4a–4b.

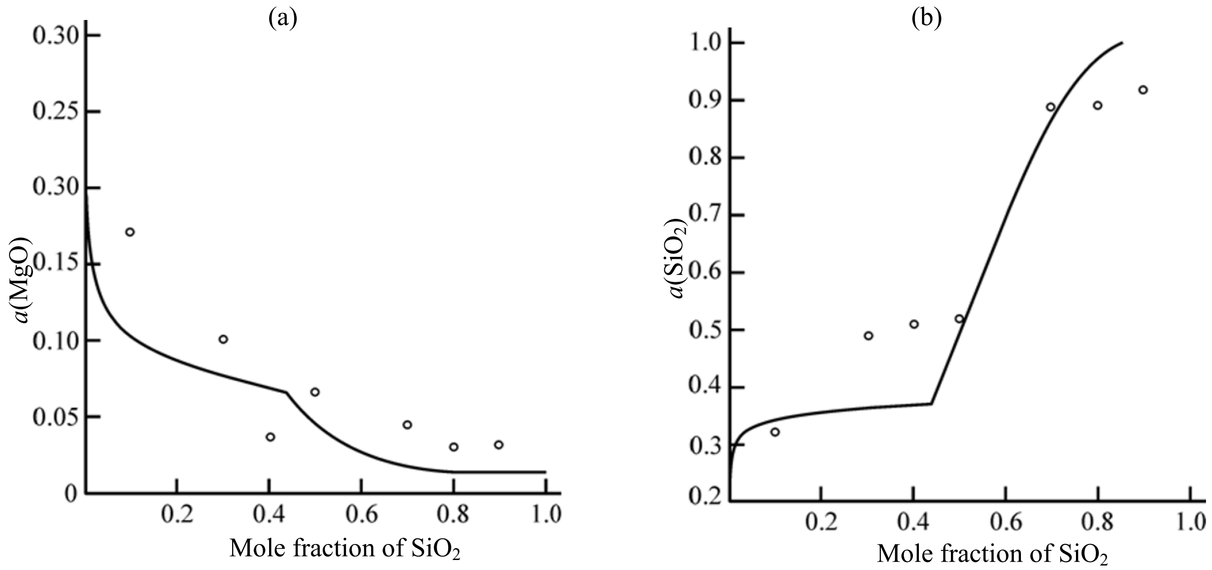

Fig. 4. Values of activities of (a) MgO and (b) SiO_2 in the system $MgO–Al_2O_3–SiO_2$ at the ratio of MgO and Al_2O_3 mole fractions 1.00 (1890 K). (Circles) experimental values, (lines) results of calculation within the limits of the Gay–Kapoor–Frohberg model.

Comparison of the found values of MgO and SiO_2 activities with the corresponding calculated values for the system $MgO–Al_2O_3–SiO_2$ (Tables 1–4, Figs. 3 and 4) and also isothermal sections of the phase diagram of the system under study at 1770, 1820, and 1890 K (Fig. 2) allows us to point out the main regularities of the thermodynamic description of phase equilibria in the system under consideration.

As is known [47], in three-phase areas of ternary systems activity of components in isothermal conditions are constant and do not vary as the system composition varies. In the monophase area activities of the components in a ternary system monotonically vary with composition. In the two-phase areas of ternary systems activity of a component varies if at least one of phases changes its composition along the section of the studied system. If the both phases have constant compositions in a ternary system, activities of components vary in discrete steps at crossing a two-phase area. In the case when a section of a ternary system coincides with a conode, activity of a component along the conode does not change. An example of the case when a conode coincides with the section SiO_2-fixed ratio [MgO]:[Al_2O_3] is the liquid-cristobalite equilibrium. Thus, the comparison of the dependences of component activities on composition, in this case on the for the composition of the ternary system $MgO–Al_2O_3–SiO_2$, with the isothermal section of the phase diagram of this system allows us to connect special features of the changes in component activities with passing three-phase, two-phase, or monophase areas.

For all MgO and SiO_2 activities determined in the present work, in the sections SiO_2-fixed ratio [MgO]:[Al_2O_3] of the studied system and the temperature range of 1770–1890 K, the presence of a horizontal piece caused by passing through the two-phase liquid-cristobalite area is characteristic. At the fixed ratios [MgO]:[Al_2O_3] of 2.33 and 1.00 the dependences of MgO and SiO_2 activities on SiO_2 concentration vary only slightly with temperature in the range 1770–1890 K. It is connected with the fact that these sections pass through the same areas of stability of phases at the specified temperatures. At the ratios [MgO]:[Al_2O_3] of 0.43 and 0.18 in the concentration region depleted of SiO_2, phase ratios vary with temperature, and it affects the dependences of MgO and SiO_2 activities on SiO_2 concentration. At 1770 K phase associates including sapphirine are stable in the system $MgO–Al_2O_3–SiO_2$, whereas at 1820 K sapphirine is unstablis and three-phase associates spinel–mullite–Al_2O_3 and a spinel–mullite–liquid are stable. At 1890 K three-phase associates spinel–Al_2O_3-liquid and mullite–Al_2O_3–liquid become stable in the studied system.

Thus, the experimental values of MgO and SiO_2 activities in the system $MgO–Al_2O_3–SiO_2$ obtained in the present work (Tables 1–4), and the results of calculation of isothermal sections of the phase diagram of this system (Figs. 2–4) fulfilled for the description of its properties within the limits of the Gay–Kapoor–Frohberg model with the use of the thermodynamic database [37–40] are in a good agreement.

EXPERIMENTAL

The work was carried out by the method of high-temperature mass spectrometry on an MS-1301 mass spectrometer at the ionizing voltage of 25 V. Molybdenum effusion cells were heated up by electronic bombing. Temperature was measured by an EOP-66 optical pyrometer. Measuring errors in the temperature range of 1800–2200 K did not exceed ±5 K. The apparatus was preliminarily calibrated by the integral method with standards of pressure. As standards of pressure we used gold [48] and CaF_2 [49].

Samples of the system $MgO–Al_2O_3–SiO_2$ were obtained by the multistage solid-phase procedure. The reagents $MgCO_3$, $Al(OH)_3$, and quartz (special-purity grade) taken in necessary proportions were ground in a jasper mortar with ethanol and dried under an infrared lamp. Then the mixtures were annealed in a KO–14 Silit furnace in air atmosphere. The samples were annealed in air in two stages: at 900°C with holding for 8 h and subsequent grinding, and for the second time at 1100°C within 8 h. Identification of the samples was carried out by X-ray analysis.

REFERENCES

1. Stolyarova, V.L., Lopatin, S.I., Shugurov, S.M., and Shilov, A.L., *Zh. Obshch. Khim*., 2010, vol. 80, no. 12, p. 1943.
2. Budnikov, P.P. and Zlochevskaya, K.M., *Dokl. Akad. Nauk SSSR*, 1964, vol. 156, no. 1, p. 158.
3. Budnikov, P.P., Balkevich, V.L., Berezhnoi, A.S., Bulavin, I.A., Kukolev, G.V., Poluboyarinov, D.N., and Popil'skii, R.Ya., *Khimicheskaya tekhnologiya keramiki i ogneuporov* (Chemical Technology of Ceramics and Refractories), Moscow: Izd. Literatury po Stroitel'stvu, 1972.
4. Tulyaganov, D.U., Ribeiro, M.J., and Labrincha, J.A., *Ceramics International*, 2002, vol. 28, no. 5, p. 515.
5. Tulyaganov, D.U., Tukhtaev, M.E., Escalante, J.I., Ribeiro, M.J., and Labrincha, J.A., *J. Eur. Ceram. Soc*., 2002, vol. 22, no. 11, p. 1775.
6. Wang, L.J., Stolyarova, V.L., Lopatin, S.I., and Seetharaman, S., *Rapid Communications in Mass Spectrometry*, 2009, vol. 23, no. 14, p. 2233.
7. Wang, H., Stolyarova, V.L., Lopatin, S.I., Kutuzova, M.E., and Seetharaman, S., *Rapid Communications in Mass Spectrometry*, 2010, vol. 24, no. 16, p. 2420.
8. *Slag Atlas*, 2nd ed., Verein Deutscher Eisenhuttenleute ed., Verlag Stahleisen GmbH, D-Dusseldorf, Germany. 1995.
9. Levin, E.M., Robbins, C.R., and McMurdie, H.F., *Phase Diagrams for Ceramists*, Columbus, Ohio, USA, 1964, vol. 1, Fig. 712.
10. Schreyer, W. and Schairer, J.F., *Amer. Mineralogist*, 1962, vol. 47, nos. 1–2, p. 90.
11. Schlaudt, Ch. M. and Roy, D.M., *J. Am. Ceram. Soc*., 1965, vol. 48, no. 5, p. 248.
12. Greig, J.W., *Am. J. Sci*., 1927, vol. 13, no. 73, p. 1.
13. Petru, Z., *Proc. Conference on Silicate Industry and Silica Science: 13. SILICONF-81 XIII,* Budapest, 1981, Pt. 1, p. 154.
14. Mazurin, O.V., Strel'tsina, M.V., and Shvaiko-Shvaikovskaya, T.P., *Svoistva stekol i stekloobrazuyushchikh rasplavov* (Properties of Glasses and Glass-forming Melts), St. Petersburg: Nauka, 1996, vol. VI, part 1.
15. Rein, R.H. and Chipman, J., *Trans. Met. Soc. AIME*., 1965, vol. 233, no. 2, p. 415.
16. Henderson, D. and Tailor, J., J. *Iron Steel Ist*., 1966, vol. 204, pt. I, p. 39.
17. Charlu, T.V., Newton, R.C., and Kleppa, O.J., *Geochim. Cosmochim. Acta*, 1975, vol. 39, no. 11, p. 1487.
18. Roy, B. N. and Navrotsky, A., *J. Am. Ceram. Soc*., 1984, vol. 67, no. 9, p. 606.
19. Kiseleva, I.A., *Geochem. Internat*., 1976, vol. 2, no. 1, p. 113.
20. Geiger, C.A. and Voigtlander, H., *Contrib. Mineral. Petrol*., 2000, vol. 138, no. 1, p. 46.
21. *High Temperature Corrosion and Materials Chemistry III*, McNallan, M. and Opila, E., Eds., Pennington: The Electrochem. Soc., 2001, vol. 12, p. 322.
22. Stolyarova, V.L., *J. Non-Crystalline Solids*, 2008, vol. 354, nos. 12–13, p. 1373.
23. Stolyarova, V.L. and Semenov, G.A., *Mass Spectrometric Study of the Vaporization of Oxide Systems*, Chichester: Wiley and Sons, 1994.
24. Schornikov, S.I., Stolyarova, V.L., and Shultz, M.M., *Rapid Communications in Mass Spectrometry*, 1994, vol. 8, no. 5, p. 478.
25. Shul'ts, M.M., Shornikov, S.I., and Stolyarova, V.L., *Dokl. Akad. Nauk*, 1994, vol. 336, no. 3, p. 368.
26. Bjorkval, J. and Stolyarova, V.L., *Rapid Communications in Mass Spectrometry*, 2001, vol. 15, no. 10, p. 836.
27. Bjorkval, J., Sichen, Du, Stolyarova, V.L., and Seetharaman, S., *Fiz. Khim. Stekla*, 2001, vol. 272, p. 200.
28. Stolyarova, V.L., Lopatin, S.I., and Bondar', V.V., *Dokl. Akad. Nauk*, 2004, vol. 399, no. 5, p. 644.

29. Bondar’, V.V., Lopatin, S.I., and Stolyarova, V.L., *Neorg. Mater.*, 2005, vol. 41, no. 4, p. 434.
30. Bondar’, V.V., Lopatin S.I., and Stolyarova, V.L., *Khim. Tekhnol.*, 2004, no. 11, p. 14.
31. Stolyarova, V.L., Lopatin, S.I., and Bondar’, V.V., *Dokl. Akad. Nauk*, 2004, vol. 399, no. 1, p. 82.
32. Arutyunyan, N.A., Zaitsev, A.I., Zaitseva, N.E., and Shakhpazov, E.H., *Dokl. Akad. Nauk*, 2005, vol. 403, no. 4, p. 471.
33. Zaitsev, A.I., Arutyunyan, N.A., Shaposhnikov, N.G., Zaitseva, N.E., and Burtsev, V.T., *Zh. Fiz. Khim.*, 2006, vol. 80, no. 3, p. 413.
34. Belton, G.R. and Fruechan, R.J., *Metall. Trans.*, 1970, vol. 1, no. 4, p. 781.
35. Kulinich, V.I., Zhilo, N.L., Kozhevnikov, G.N., Mizin, V.G., and Ostrovskii, J.I., *Metally,* 1985, no. 2, p. 36.
36. Vinograd, V.L., Winkler, B., Putnis, A., Kroll, H., Milman, V., Gale, J.D., and Fabrichnaya, O.B., *Molecular Simulation*, 2006, vol. 32, no. 2, p. 85.
37. Jung, I.H., Decterov, S.A., and A.D. Pelton, A.D., *J. Phase Equiibria and Diffusion*, 2004, vol. 25, no. 4, p. 329.
38. Mao, H., Fabrichnaya, O., Selleby, M., and Sundman, B., *J. Mater. Res.*, 2005, vol. 20, no. 4, p. 975.
39. Fabrichnaya, O., Costa e Silva, A., and Aldinger, F., *Z. Metallkunde*, 2004, vol. 95, no. 9, p. 793.
40. Hillert, M., *J. Alloys Comp.*, 2001, vol. 320, no. 2, p. 161.
41. *Energii razryva khimicheskikh svyazei. Potentsialy ionizatsii i srodstvo k elektronu: Spravochnik* (Energies of Breaking Chemical Bonds: Ionization Potentials and Electron Affinities: Handbook), Kondrat’ev, V.N., Ed., Moscow: Nauka, 1974.
42. Huang, W., Hillert, M., and Wang, X., *Metall. Mater. Trans.*, 1995, vol. 26A, no. 9, p. 2293.
43. Dumitrescu, L. and Sundman, B., *J. Eur. Ceram. Soc.*, 1995, vol. 15, no. 3, p. 239.
44. Hallstedt, B., *J. Am. Ceram. Soc.*, 1992, vol. 75, no. 6, p. 1497.
45. Fine, H. and Gaskell, D.R., *Second International Symposium on Metallurgical Slag and Fluxes*, Lake Tahoe: TMS-AIME, 1984, p. 345.
46. *Chemical Metallurgy of Iron and Steel*, Kubaschewski, O., Ed., London, 1971, p. 17.
47. DeHoff, R., *Thermodynamics in Materials Science*, Boca Raton: CRC Press Taylor and Francis Group, 2006.
48. Paule, R.C. and Mandel, J., *Pure Appl. Chem.*, 1972, vol. 31, no. 3, p. 371.
49. Zaitsev, A.I., Korolev, N.B., and Mogutnov, B.M., *Teplofiz. Vys. Temp.*, 1989, vol. 27, no. 3, p. 465.